Biogeosciences Discuss., 11, 13389–13432, 2014
www.biogeosciences-discuss.net/11/13389/2014/
doi:10.5194/bgd-11-13389-2014

Biogeosciences Discussions
Open Access

Sourcing the iron in the naturally-fertilised bloom around the Kerguelen Plateau: particulate trace metal dynamics

P. van der Merwe[1], A. R. Bowie[1,2], F. Quéroué[1,2,3], L. Armand[4], S. Blain[5,6], F. Chever[3,7], D. Davies[1], F. Dehairs[8], F. Planchon[3], G. Sarthou[9], A. T. Townsend[10], and T. Trull[1,11]

[1]Antarctic Climate and Ecosystems CRC, University of Tasmania, 7004, Australia
[2]Institute for Marine and Antarctic Studies, University of Tasmania, Battery Point, TAS 7004, Australia
[3]Université de Brest, LEMAR, IUEM; Technopôle Brest Iroise, Place Nicolas Copernic, 29280 Plouzané, France
[4]Department of Biological Sciences and Climate Futures at Macquarie University, North Ryde, NSW 2109, Australia
[5]Sorbonne Universités, UPMC Univ Paris 06, UMR7621, Laboratoire d'Océanographie Microbienne, Observatoire Océanologique, 66650 Banyuls/mer, France
[6]CNRS, UMR7621, Laboratoire d'Océanographie Microbienne, Observatoire Océanologique, 66650 Banyuls/mer, France
[7]Ocean and Earth Science, National Oceanography Centre Southampton, University of Southampton, Southampton, SO14 3ZH, UK

[8]Vrije Universiteit Brussel, Analytical, Environmental and Geo-Chemistry & Earth System Sciences research group, Brussels, Belgium
[9]CNRS, Université de Brest, IRD, Ifremer, UMR 6539 LEMAR, IUEM; Technopôle Brest Iroise, Place Nicolas Copernic, 29280 Plouzané, France
[10]Central Science Laboratory, University of Tasmania, Sandy Bay, TAS, 7005, Australia
[11]Commonwealth Scientific and Industrial Research Organisation, Marine and Atmospheric Research, GP.O. Box 1538, Hobart, Tasmania, Australia

Received: 26 August 2014 – Accepted: 26 August 2014 – Published: 18 September 2014

Correspondence to: P. van der Merwe (pvander@utas.edu.au)

Published by Copernicus Publications on behalf of the European Geosciences Union.

Abstract

The KEOPS2 project aims to elucidate the role of natural Fe fertilisation on biogeochemical cycles and ecosystem functioning, including quantifying the sources and processes by which iron is delivered in the vicinity of the Kerguelen Archipelago, Southern Ocean. The KEOPS2 process study used an upstream HNLC, deep water (2500 m), reference station to compare with a shallow (500 m), strongly fertilised plateau station and continued the observations to a downstream, bathymetrically trapped recirculation of the Polar Front where eddies commonly form and persist for hundreds of kilometres into the Southern Ocean. Over the Kerguelen Plateau, mean particulate (1–53 µm) Fe and Al concentrations (pFe = 13.4 nM, pAl = 25.2 nM) were more than 20-fold higher than at an offshore (lower-productivity) reference station (pFe = 0.53 nM, pAl = 0.83 nM). In comparison, over the plateau dissolved Fe levels were only elevated by a factor of ∼ 2. Over the Kerguelen Plateau, ratios of pMn / pAl and pFe / pAl resemble basalt, likely originating from glacial/fluvial inputs into shallow coastal waters. In downstream, offshore deep-waters, higher pFe / pAl, and pMn / pAl ratios were observed, suggesting loss of lithogenic material accompanied by retention of pFe and pMn. Biological uptake of dissolved Fe and Mn and conversion into the biogenic particulate fraction or aggregation of particulate metals onto bioaggregates also increased these ratios further in surface waters as the bloom developed within the recirculation structure. While resuspension of shelf sediments is likely to be one of the important mechanisms of Fe fertilisation over the plateau, fluvial and glacial sources appear to be important to areas downstream of the island. Vertical profiles within an offshore recirculation feature associated with the Polar Front show pFe and pMn levels that were 6-fold and 3.5-fold lower respectively than over the plateau in surface waters, though still 3.6-fold and 1.7-fold higher respectively than the reference station. Within the recirculation feature, strong depletions of pFe and pMn were observed in the remnant winter water (temperature-minimum) layer near 175 m, with higher values above and below this depth. The correspondence between the pFe minima and the winter water

BGD
11, 13389–13432, 2014

temperature minima implies a seasonal cycle is involved in the supply of pFe into the fertilized region. This observed association is indicative of reduced supply in winter, which is counterintuitive if sediment resuspension and entrainment within the mixed layer is the primary fertilising mechanism to the downstream recirculation structure. Therefore, we hypothesise that lateral transport of pFe from shallow coastal waters is strong in spring, associated with snow melt and increased runoff due to rainfall, drawdown through summer and reduced supply in winter when snowfall and freezing conditions predominate in the Kerguelen region.

1 Introduction

Small scale fertilisation experiments have now clearly established that Southern Ocean primary production is limited by the availability of the micronutrient iron (Fe) (Boyd et al., 2007; de Baar, 2005). This limitation on the biological pump means that the Southern Ocean does not realise its full potential in transferring atmospheric CO_2 into the ocean interior; a result illustrated in sedimentary records over geological timescales and supported by modelling studies (Bopp et al., 2003; Martin, 1990; Watson et al., 2000). Less well understood is the overall system response to the addition of Fe as efficiency estimates (defined here as the amount of carbon exported relative to Fe added above baseline conditions) can vary by an order of magnitude (Blain et al., 2007; Pollard et al., 2009; Savoye et al., 2008). Both the original and subsequent KEOPS missions aimed to resolve not only the efficiency estimate, but also the response of the ecosystem and the overall effect on biogeochemical cycles due to natural Fe fertilisation in the vicinity of the Kerguelen plateau. The KEOPS natural fertilisation experiment is complementary to artificial Fe enrichment experiments due to the fact that its scale is much larger and timeframe longer than what is currently feasible in artificial fertilisation experiments. Furthermore, due to the sustained release of Fe into the fertilised region, as opposed to a sudden pulse artificial experiment, the technical challenges of monitoring carbon export are reduced. Furthermore, there is growing evidence that sustained

BGD
11, 13389–13432, 2014

Fe fertilisation favours large, highly silicified, slow growing diatoms that are efficient at exporting carbon into the ocean interior (Quéguiner, 2013). When the results of process studies such as KEOPS are extrapolated over the whole Southern Ocean, a small change in the efficiency estimate could result in different conclusions as to the efficacy, for instance, of artificial Fe fertilisation as a means of mitigating rising atmospheric concentrations of anthropogenic CO_2.

Dissolved Fe (< 0.2 µm) is traditionally identified as the size fraction that is available for biological uptake (de Baar and de Jong, 2001), and as such, the larger particulate fraction (> 0.2 µm) is often less studied. However, the particulate fraction can yield important information for several reasons; firstly the dissolved fraction is constantly in a state of change with uptake, particle scavenging and remineralisation occurring simultaneously and at varying rates depending on many factors including complexation with organic ligands (Johnson et al., 1997) and the biological community present (Sunda, 2001). Thus, interpretation of dFe data is difficult without a rarely-obtained perspective on the time varying aspects of the dFe distribution. Secondly, as a fraction of the total Fe, the major sources of Fe into fertilised regions (e.g. continental bed rock weathering, resuspension of authigenic sediments, atmospheric and extra-terrestrial dust) are small particles (> 0.2 µm), with the concentration being more stable over weeks to months, due to its abundance and relatively slow biological uptake. The particulate fraction is primarily lost from surface waters through sinking, either directly or via adhesion to bioaggregates (Frew et al., 2006). However, there is a constant transfer of dissolved Fe to particulate Fe, either via biological uptake or precipitation and, particulate Fe to dissolved Fe, via dissolution and biologically mediated processes (Moffett, 2001). Thus, the particulate fraction that is small enough to avoid sinking out of the water column rapidly (0.2–5 µm) can be considered as a significant source of dissolved Fe, with the rate of supply into surrounding waters dependent on the dissolution and leaching rate. Furthermore, there is growing evidence that particles in this size fraction are readily produced by mechanical erosion of bedrock due to glacial processes at high

BGD
11, 13389–13432, 2014

latitudes and that this large source may be partially bioavailable (Hawkings et al., 2014; Poulton and Raiswell, 2005; Raiswell et al., 2008a, b, 2006a).

The first KEOPS process study was conducted in 2005 and specifically focused on processes affecting the demise of the Spring bloom over the Kerguelen Plateau (Blain et al., 2007). The findings included determining Fe principally activated increased primary production in the area (Blain et al., 2007; Chever et al., 2009). From the data gathered it was proposed that resuspension of plateau-derived sediments and entrainment into the mixed layer during increased wind mixing that deepened the mixed layer, was the primary source of particulate and subsequently, dissolved Fe to the downstream blooms. Resolution of the Fe budget (accounting for all sources and sinks of Fe in the system), from observations made during the first mission, found that the vertical supply of dissolved Fe was not sufficient to supply phytoplankton demand. Blain et al. (2007) closed the KEOPS Fe budget by assuming that dissolution of a small fraction of the unconstrained particulate Fe pool must occur. The KEOPS2 mission aimed to improve on the successes of the first process study by accounting for the missing Fe in the budget, namely particulate Fe (pFe). Thus, we aim to test the KEOPS1 hypothesis that unconstrained particulate Fe is the missing Fe of the KEOPS Fe budget by documenting the particulate metal enrichment around the Kerguelen plateau. Our goal is to determine the sources of Fe enrichment within areas of interest (i.e. reference, plateau and the recirculation structure, see Fig. 1). Together with trace metal analysis of suspended particles, underlying sediment and settling particulate material will be analysed to elucidate the source to sink progression of Fe pools. Following on from this work, and together with dissolved Fe measurements (Quéroué et al., 2014), a focused Fe budget will be constructed (Bowie et al., 2014).

BGD
11, 13389–13432, 2014

2 Methods

2.1 In situ pumps (ISP)

All sample handling, processing and preparation was performed in accordance with general GEOTRACES protocols (http://www.geotraces.org/) and specific methodologies outlined in Bowie et al. (2010). Briefly, suspended particles were collected using up to 11 in situ pumps (ISPs) (McLane WTS and Challenger) suspended simultaneously at varying depths throughout the water column. Depths were chosen after viewing conductivity, temperature and depth (CTD) data to sample within oceanographic features of interest as well as obtaining a representative full water column profile. The ISPs were fitted with, 142 mm quartz micro fibre (QMA) (Sartorius) filters with 53 µm nylon pre-filters and 350 µm polyester supports (all filters and supports were pre-combusted to remove particulate organic carbon and then acid-washed with Seastar Baseline™ HCl and rinsed with copious amounts of ultra-pure water). Both the nylon prefilter and QMA filter were analysed for every pump giving two size fractions at each sampling location. Therefore, all particles greater than 53 µm were collected on the prefilter and all particles within the 1–53 µm size range were collected on the underlying QMA filter. Lithogenics sourced from bedrock or sediments in the larger size range (> 53 µm) would have a high sinking velocity (> 500 m day^{-1}) according to Stokes law and as such would be expected to make up a relatively small fraction of the total particles in this size range. In comparison, the 1–53 µm size class can potentially capture both small biogenic and lithogenic particles. This is due to the prediction that small lithogenic particles (1–5 µm) have significantly slower sinking rates (0.1–10 m day^{-1}) than large lithogenic particles according to Stokes law.

The ISPs were programmed to pump for up to four hours, allowing up to 2000 L of seawater to be filtered. After retrieval, the filters were bagged and processed within an ISO class 5, containerised clean room. Replicate 14 mm punches were taken using an acid-washed polycarbonate punch and stored frozen at −18 °C until analysis at the

BGD
11, 13389–13432, 2014

home laboratory. The 14 mm punches were then used for particulate metal analysis, particulate organic carbon and particulate organic nitrogen analysis.

2.2 Sediment traps (Technicap PPS3/3)

For a full description of the sediment trap data during KEOPS2 see Laurenceau et al. (2014) and Bowie et al. (2014). Two Technicap PPS3 free-floating sediment traps were deployed below the mixed layer at a depth of 200 m. The two sediment traps were deployed twice, giving a total of 4 deployments. The traps were prepared with acid-cleaned sampling cups containing low-trace-metal brine solution (salinity ~ 60). The trap was programmed to sample for 1.5 to 5.5 days, whilst the 12 individual sampling containers were open for an equal portion of the total deployment. Upon retrieval, the sampling containers were removed from the carousel, sealed and processed within an ISO class 5, containerised clean room. The samples were filtered onto acid-washed, 2 µm polycarbonate membrane filter via a 350 µm nylon pre-filter using a Sartorius™ PTFE filtration unit. The 350 µm pre-filter was selected to exclude large copepods and other large plankton that would lead to unrealistic sample variability.

2.3 Sediment coring

An Oktopus Multicorer (www.oktopus-mari-tech.de) was used to collect 8 replicate, 610 mm × 95 mm sediment cores, simultaneously within a 1 m^2 area at each station. The uppermost 5 mm of surface sediment was subsampled according to Armand et al. (2008) representing an approximate sedimentation period of < 1000 years.

2.4 Analysis

2.4.1 ISP filters for particulate metals

All digestions and evaporations were carried out within a digestion hood (SCP Science), where air was HEPA filtered during intake and subsequently extracted

BGD
11, 13389–13432, 2014

through a fume hood. Filter blanks and sample filters were digested in 15 mL acid cleaned, Teflon perfluoroalkoxy (PFA) screw cap vials (Savillex™) using ultra-pure nitric acid (1 mL 16 M HNO_3) (Seastar Baseline™) heated to 120 °C for 12 h on a Teflon coated hotplate (SCP Science DigiPREP™), following the method outlined in Bowie et al. (2010). Blanks containing only HNO_3 were also analysed to determine the contribution of the digestion acid without filter material. No hydrofluoric acid (HF) was used during the digestion as it was incompatible with the QMA filters used by the ISPs. QMA filters were chosen as they could be acid cleaned to a trace-metal-clean level and the filter material allowed high particle loading and low wash-off upon collection. Furthermore, the filters were compatible for use with both Inductively Coupled Plasma Mass Spectrometry (ICP-MS) and elemental (CHN) analysis. The digest solution was diluted with 10 mL of ultra-high purity water and spiked with 10 ppb indium as an internal standard. Samples were analyzed by Sector Field ICP-MS (Finnigan Element II, Thermo Scientific) (Cullen and Sherrell, 1999; Townsend, 2000). The data were quality controlled by comparison with a certified reference material with a similar composition to the material collected (BCR-414 trace metals in phytoplankton, European Commission).

2.4.2 Sediment analysis for particulate metals

Digestions and analysis were performed as per the ISP filters except that HF acid was used to digest these highly refractory samples. The HNO_3 digest used for the ISP filters is relatively weak but digests the biogenic fraction completely as evidenced by the excellent recoveries on the BCR414 certified reference material (trace metals in phytoplankton) (Table A1) but has limited recoveries of the lithogenic fraction as evidenced by the low recoveries of pAl and pTi in MESS-3 and PACS-2 sediment certified reference material (Bowie et al., 2010).

During the HF digest, a mixture of strong acids (250 µL HNO_3, 250 µL HF and 500 µL HCl) were used as per Bowie et al. (2010). After 12 h at 95 °C the digest PFA vials were uncapped and evaporated to dryness at 60 °C for 4 h. The digest was then resuspended

BGD
11, 13389–13432, 2014

in 10 % HNO_3 with 10 ppb indium added as internal standard. A 100× dilution factor was considered sufficient to place the ∼ 20 mg sediment samples within the calibration range of the SF-ICP-MS.

2.4.3 Particulate organic carbon (POC) and nitrogen (PN)

All glassware in contact with POC samples was pre-combusted prior to field work (450 °C for 12 h). Total nitrogen, carbon and hydrogen were determined at the Central Science Laboratory, University of Tasmania, using a Thermo Finnigan EA 1112 Series Flash Elemental Analyzer (estimated precision ∼ 1 %).

3 Results and Discussion

3.1 Station-types

The sampling locations of KEOPS2 (Fig. 1) were designed to capture the key regime types of the Kerguelen Archipelago (Blain et al., 2014b) including the high nutrient, low chlorophyll (HNLC) reference waters (station R-2), the high-trace-metal plateau waters (station A3), the northern Polar Front (station F-L) and a quasi-stationary, bathymetrically trapped recirculation structure (E-1, E-3 and E-5) to the east of Kerguelen Island (Table 1). Stations E-1, E-3 and E-5 can be thought of as a pseudo-Lagrangian time series. In addition, two stations were sampled at the eastern and western extremes of the recirculation structure (E-4W and E-4E) which proved to contrast in absolute concentrations as well as elemental ratios of particulate trace metals.

3.2 Surface water flow around the Kerguelen Plateau

During KEOPS1, van Beek et al. (2008), Zhang et al. (2008) and Chever et al. (2009) revealed that the water column southeast of Kerguelen Island was modified by passing over the Heard Island Plateau. Park et al. (2008) demonstrated that the interaction of

BGD
11, 13389–13432, 2014

the water masses over the Kerguelen Plateau could be divided into the southern and northern water masses separated by the Polar Front (PF) (Fig. 1). The southern water mass has source waters being derived from the Antarctic surface waters (AASW), southwest of Kerguelen which is bound to the north by the shallow bathymetry of the Leclaire Rise. These surface waters are generally colder and saltier than to the north (Fig. 2). The AASW also flows around Heard Island and a weaker surface current flows northwest over the Kerguelen Plateau towards the north east of Kerguelen Island where it is bound to the north by the PF. This cold surface current can be seen during winter in Fig. 2. The northern water mass has a source of easterly flowing Sub Antarctic Surface Waters (SASW). The portion of the SASW that interacts with Kerguelen Island is termed Kerguelen Island source waters and is bound to the south by the PF (Fig. 2). A broad and poorly defined mixing zone to the east of Kerguelen Island has been identified at the junction of these southern and northern water masses. As a result of the mixing, eddies commonly form in this region. Also within this mixing zone, surface filaments, identified by elevated Chlorophyll *a*, can be seen in SeaWiFS images diverging from the PF and entering the eastern boundary of the recirculation structure (see Supplement in Trull et al., 2014).

The Kerguelen Archipelago is isolated, being a relatively small and localised source of Fe fertilisation surrounded by the large and deep, HNLC, low Fe, Southern Ocean. Therefore, when identifying an Fe source to the region, our focus is on the plateau and the two islands, Kerguelen and Heard. Over geological timescales, all pFe distributed throughout the water column within this region must be derived from all forms of weathering of bed rock including, fluvial and glacial outflow as well as dust from the islands, hydrothermal and extra-terrestrial input. Over shorter time frames, shelf sediments in the region are a form of recycled Fe as the vast majority of these sediments are a combination of siliceous ooze (Armand et al., 2008) and glacio-marine sediments; the exported product of the highly productive overlying waters together with some lithogenics (sourced from bed-rock) that were unutilised or non-bioavailable and fast-sinking. Therefore, understanding the pathways of supply of this new Fe is impor-

BGD
11, 13389–13432, 2014

tant to understanding the processes controlling the long term productivity and therefore, carbon sequestration, in the area.

3.3 Underlying sediment analysis

Analysis of sediments sourced from cores taken at each station revealed a distinctly different sediment signature at station R-2 compared with any other station (Table 2). The reference station signature was approximately six times enriched in Mn relative to Al (Mn : Al 0.063) in comparison to the plateau station (A3) (Mn : Al 0.011). The Mn : Al sedimentary signature at A3 was almost identical to authigenic sediments previously reported from the Amundsen Sea (Angino, 1966). We consider the enriched Mn at R-2 could be due to either MnO_2 enrichment in the surface sediments during redox cycling of early diagenesis (Planquette et al., 2013), or supplied via a Mn enriched source such as hydrothermal venting near the Leclaire Rise. The extremely low carbon content of the sediment at station R-2, as evidenced by its near white colour, low diatom content (Armand, pers. obs.) and low carbon export flux (Laurenceau et al., 2014; Planchon et al., 2014), suggests that MnO_2 enrichment in the surface sediments during redox cycling is more likely at R-2.

The authigenic sediment ratio of Fe : Al was lower at station R-2 (Fe : Al = 0.73) in comparison to any other station (Fe : Al range 0.81–1.1). However, all of our observed pFe : pAl ratios were higher than upper crustal ratios (Fe : Al 0.2) or Amundsen Sea surface sediments (Fe : Al 0.26) (Angino, 1966). Interestingly, our observed pFe : pAl sedimentary ratios were similar to the ratio found in phytoplankton such as the BCR-414 certified reference material (freshwater phytoplankton) (Fe : Al = 1.01) used in this study (Table A1). Furthermore, the pFe : pAl ratio of sinking particles captured by the free floating PPS3 sediment traps (marine snow) had similar ratios of pFe : pAl of 1.02, 1.05, 0.91 and 0.70 for stations E-1, E-3, E-5 and A3–2, respectively (Table 3). These observations highlight the major contribution of sinking biogenic material to the authigenic sediments in the area around the Kerguelen Plateau which was in contrast to the signature at station R-2 due to its low productivity. The pFe in the sediments at all

BGD
11, 13389–13432, 2014

stations and primarily at station R-2 (as a fraction of its total weight) were similar to Weddell Sea surface sediments (Angino and Andrews, 1968) which ranged from 0.9–3.2 %. In comparison, station R-2 has a mean value of 0.1 % Fe while station E-3, A3, F-L and E-4W had mean values of 0.3, 0.8, 1.5 and 2.5 % respectively. The low fraction of Fe within the authigenic sediment at R-2 indicates limited pFe supply at this station in comparison to either the Weddell Sea or the Kerguelen Plateau presented here.

3.4 Plateau, reference and polar front stations

Station A3, located over the Kerguelen Plateau, has a bottom depth of 527 m, making it the shallowest station sampled for trace metal analysis of suspended particles and one of the most likely to be influenced by resuspension of shelf sediments (Fig. 1). The proximity of the station to Heard and Kerguelen Island (roughly half way between the two) means that fluvial and glacial runoff may also drive fertilisation at this site. However, the hydrography of the area dictates that Heard Island is upstream of A3 and Kerguelen Island is downstream (Zhou et al., 2014). In contrast, the reference station (R-2) has a bottom depth of 2528 m and is characterised by low surface Chl *a* concentrations (Lasbleiz et al., 2014) and nutrient concentrations characteristic of HNLC waters (Blain et al., 2014a). Station F-L is approximately 313 km northeast of Kerguelen Island with a bottom depth of 2690 m and represents the northern PF. Station F-L is downstream of Kerguelen Island, with the PF delivering waters that originated near station R-2. In this case, the waters crossing Station F-L have interacted with both the plateau and shallow coastal waters of Kerguelen Island.

The pFe, pAl and pMn concentrations at the reference station (R-2) only increase slightly towards the sea floor; however, enrichment in pFe, pAl and primarily pMn is evident at 500 m likely due to proximity to the Leclaire Rise (Fig. 3) (discussed in detail below). The northern PF station (F-L) exhibits moderate concentrations of pFe, pAl and pMn throughout the water column, somewhat higher than the reference station, and much higher concentrations are observed in close proximity to the sea floor. It should be noted that the deepest sample at R-2 was 148 m above the seafloor, while

BGD
11, 13389–13432, 2014

at F-L it was only 90 m above the sea floor and this could well explain the observed difference, given the strong decrease of nepheloid layers away from the seabed (Blain et al., 2007; Jouandet et al., 2014).

Profiles of pFe and pAl in the 1–53 um size range from station R-2, A3 and F-L are shown in Fig. 3. The plateau station (A3) was sampled twice during the study (A3–1 and A3–2), separated by 20 days. Surface chlorophyll images revealed that between visits to the site, a large bloom developed in the vicinity and extended over the site, and was beginning to fade again by the time of the second sampling (Trull et al., 2014). Thus, station A3–1 can be thought of as pre-bloom and A3–2 as post-bloom conditions. Particulate Fe, Al and Mn generally increased towards the sea floor at station A3, with the exception of a slight enrichment below the mixed layer during the second visit (A3–2) to the station in the > 53 µm size fraction (Fig. 4). To investigate the progression of pFe through time, we integrated the pFe throughout the full water column, and observed a decrease in the pFe stock from 9.1 to 4.5 mmol m^{-2} between the first and second visit to station A3. This translates to a 51 % reduction in pFe for all size classes combined (i.e. > 1 µm). However, if we look closer at the pFe distribution only within the surface mixed layer (165 m) between A3–1 and A3–2, we observe a loss of 70 % of the integrated total pFe (> 1 µm) (Fig. 4). Concurrently, using an Underwater Vision Profiler to track particle size distribution, Jouandet et al., (2014) noted a 4 fold increase in particle numerical abundance through the full water column. Their one dimensional particle dynamic model supported the hypothesis that the increase in biogenic particles, due to blooming conditions, resulted in the rapid formation of large particles due to coagulation and subsequent vertical transport to the base of the mixed layer. This result is supported in the current data set, in that we see a large decrease in small pFe particles within the mixed layer and a moderate increase in large pFe particles at the base of the mixed layer when comparing pre (A3–1) to post (A3–2) bloom conditions (Fig. 4).

Thus, it appears that physical aggregation within the mixed layer of the particles onto biogenic phyto-aggregates during the bloom development and export to the base of

BGD
11, 13389–13432, 2014

the mixed layer, combined with significantly lower concentrations above the seafloor resulted in the observed 51 % reduction in pFe (> 1 µm) between A3–1 and A3–2. The significantly lower concentration at 440 m during the post-bloom conditions of A3–2 may be due to increased small particle scavenging resulting from sinking phyto-aggregates or alternatively, small-scale variation in the thickness of the nepheloid layer.

3.5 Elemental ratios at stations R-2, F-L and A3

As station A3 is located over the Kerguelen Plateau and also is in close proximity to fluvial and glacial runoff from Heard Island, we would expect the trace metal source signature of suspended particles to be unique here in comparison to our reference (R-2) and PF (F-L) stations. The particles over the Kerguelen Plateau were characterised by very high pFe (0.94–30.4 nM) and pAl (1.5–58.6 nM) with concentrations an order of magnitude higher than R-2 (<DL-1.35 nM Fe and <DL-2.08 nM Al). The reference station was characterised by low surface Chl *a* concentrations characteristic of HNLC waters (Lasbleiz et al., 2014), however, it is relatively close to the Leclaire Rise; a seamount with its shallowest point 135 km west northwest of station R-2 rising up to approximately 395 m. The Leclaire Rise extends to 70 km northwest of station R-2 where it reaches a depth of approximately 550 m. It is important to recall in this context that the PF divides the northeast flowing AASW from the eastward flowing SASW to the north (Park et al., 2008). Classical theory suggests that this oceanographic feature should block much of the enrichment from the Leclaire Rise to station R-2. However, enrichment was evident in the vertical profiles of pFe, pMn and pAl at station R-2 at 500 m depth (Fig. 3).

Figure 5 illustrates the full water column elemental ratios at the reference station (R-2) in comparison to the Kerguelen Plateau stations (A3–1 and A3–2) and reveals that Mn : Fe as well as Ba : Al are strikingly unique. At station R-2, below 500 m, we see Mn : Fe 2× higher than A3, Mn : Al 4.5× higher and Ba : Al ratios 10× higher than at A3, making this source signature relatively clear (Table 4). The unique ratios are considered a combination of extremely high pFe and pAl supply over the Kerguelen

BGD
11, 13389–13432, 2014

Plateau that is relatively deficient in pMn such as would be found in glacial runoff that has a signature which reflects fresh weathering of basaltic rocks (Doucet et al., 2005). Furthermore, a source of dissolved or particulate Mn, uncoupled from pFe and pAl from the Leclaire Rise could alter the elemental ratios as observed. This source theory is supported by the observation of high dissolved Mn (dMn) near the Leclaire Rise (Quéroué et al., 2014) and uniquely high pMn : pFe in sediments found below station R-2 (Table 2). Surface water particulate trace metals also reveal distinct differences. The ratios of pFe : pAl, pMn : pAl and pMn : pFe all increase from the bottom of the mixed layer to the surface at stations R-2 and F-L (Fig. 5). This profile characteristic is in contrast to stations A3–1. The observed modification of the elemental ratios in the surface mixed layer at R-2 and F-L is most likely due to biological uptake of dissolved trace elements and conversion into the biogenic particulate fraction.

Particulate Al and pFe were closely coupled across all stations (Spearmans RHO $R = 0.91$ $P < 0.01$ $n = 70$). However, pAl and pMn, although still strongly correlated ($R = 0.80$ $P < 0.01$ $n = 70$), appeared more variable than pFe vs. pAl. Figure 6 illustrates this variability in the pMn in comparison to pAl as a function of its location within the study area. The observed variability in pMn but not pFe relative to pAl highlights the uncoupling between some of the sources of pMn and pFe. Specifically, the observed variability points to a uniquely high Mn : Fe source either in the authigenic sediments of the Leclaire Rise and/or a hydrothermal source (German et al., 1991), or a process whereby pAl is preferentially stripped out with distance from the source. A study by Shigemitsu et al. (2013) showed that the concentration of pAl in suspended particulate material in the Intermediate Water of the Sea of Okhotsk (western Pacific Ocean), decreased with distance from the shelf source preferentially in relation to pFe and pMn. They concluded that increasing pFe : pAl and pMn : pAl ratios occurred with distance from the source and suggested that the denser, lithogenic particles settled out preferentially, stripping out pAl. Furthermore, they found pFe, associated with organic matter, remained suspended in the water column more readily than pAl. These processes could explain the observed modification of the elemental ratios between stations R-2,

BGD
11, 13389–13432, 2014

A3 and possibly F-L. The stations that were in close proximity to the shelf source such as A3–1 and A3–2 were indeed enriched in lithogenic pAl and as such pFe : pAl was relatively low (Fig. 5). In contrast, F-L was at the greatest distance from a sedimentary source and displayed the highest pFe : pAl ratio, whereas station R-2, being relatively close to the Leclaire rise, had an intermediate ratio.

3.6 What are the sources of particulate trace metals over the plateau and downstream?

The high particulate trace metal concentrations found at 440 m, at A3–1 and A3–2, near the sea floor, most likely originated from resuspension of deep (~ 500 m) shelf sediments. The cause of the variability between A3–1 and A3–2 at this depth remains unclear, but could reflect small scale variability in the depth of the nepheloid layer or be the result of temporal variability due to the action of tides and internal waves (McCave, 1986). The pMn : pAl, pMn : pFe and pBa : pAl ratios for A3–1 and A3–2 are similar from the sea floor to the approximate base of the surface mixed layer, with values higher than the mean crustal ratios (Taylor and McLennan, 1985), but lower than either basalt (Doucet et al., 2005) or the underlying sediment ratios (Table 2). Within the surface mixed layer, A3–1 maintains similar ratios to the deep water column, while at A3–2 the ratios diverge towards the surface. The particulate trace metal signature within the mixed layer at A3–2 increases in pMn and pBa relative to pAl, which likely results from particle scavenging and settling of Al rich, refractory lithogenics as outlined above (Sect. 3.4).

Glacial flour is the result of mechanical erosion of bed rock by glaciers. Typical particle sizes are within the silt size range but can overlap with clays (0.002–0.063 mm). Recent research suggests that Fe sourced from glacial erosion can be a major source of bioavailable Fe to the Southern Ocean (Poulton and Raiswell, 2005; Raiswell et al., 2008a, b, 2006b). Assuming no mixing and a dilute suspension, Stoke's law predicts that the small grain size of glacial flour allows it to remain suspended within a 500 m water column for between 2 and 2500 days or within a 165 m mixed layer for 1 to

BGD
11, 13389–13432, 2014

831 days depending on particle size. Certainly, mixing within the surface mixed layer would increase this duration significantly, meaning that glacial and fluvial input from both Heard and Kerguelen Island could remain suspended in the mixed layer for long enough to travel well past any of the stations in the present study. Furthermore, it has been shown that 2–3 % of glacial flour is directly soluble and therefore bioavailable (Schroth et al., 2009). It is thought that this soluble fraction is leached from glacial flour over time (Raiswell et al., 2010) following an exponential decay (Raiswell, 2011), so it is possible that this source could be excluded from the < 0.2 µm dissolved fraction, but included in the 1–53 µm particulate fraction presented here. This is especially true of nanoparticulate Fe that is attached to the surface of larger sediment grains as has been observed previously in glacial sediments (Shaw et al., 2011). Given that the particulate fraction is generally an order of magnitude higher in concentration than the dissolved fraction, this source may well be more significant in stimulating phytoplankton blooms than previously estimated. Overall, station A3 appeared to be directly fertilised by resuspension of shelf sediments at depth, and entrainment of this pFe-rich water occurred during events that deepen the mixed layer periodically. However, lateral supply above the mixed layer of small particles from shallow coastal sources around Heard Island, including glacial melt waters, cannot be ruled out.

3.7 Biogenic and sedimentary particulate trace metals

If we assume that all particulate phosphorus (pP) is of biogenic origin, we can calculate the biogenic Fe and Mn fraction of the total Fe and Mn concentration by normalising to pP and comparing with published elemental ratios of Southern Ocean diatoms (Planquette et al., 2013). For the calculations we used the upper limit of Fe : P (1.93 mmol mol^{-1}) and Mn : P (0.42 mmol mol^{-1}) reported by Twinning et al. (2004) for Southern Ocean diatom assemblages. Given that pP and POC are remineralised throughout the water column and are generated within the surface mixed layer, calculations of biogenic trace metals will only be valid within the surface mixed layer, as the concentration of pP and POC decreases strongly with depth. Figure 3 illustrates

BGD
11, 13389–13432, 2014

the contribution of biogenic Fe in surface waters at stations R-2, A3 and F-L. The biogenic Fe and Mn (data not shown) fractions within the surface mixed layer correlate with POC (Spearmans RHO, $R = 0.75$ $P < 0.01$ and $R = 0.85$ $P < 0.01$, respectively). Station R-2 and F-L have biogenic Fe fractions that are higher near the surface than at depth (Fig. 3). In contrast, at stations A3–1 and A3–2, biogenic Fe and Mn only make up a relatively small fraction of the total pFe throughout the water column although at station A3–2 we see a slight increase in biogenic pFe towards the surface, corresponding with the development of a bloom. Biogenic Fe at stations A3–1 and A3–2 constitutes less than 1 and 5 % respectively of the total Fe. The low biogenic fraction at station A3–1 most likely results from an excess of lithogenic Fe, Al and Mn to the water column from the shelf sediments as well as fluvial/glacial runoff from nearby Islands of the Kerguelen Archipelago, which are in excess to demand. A similar pattern was observed during a study located in the Amundsen Sea (Planquette et al., 2013) where the percentage of biogenic Fe and Mn (full water column mean) reduced with proximity to the trace metal source.

Alternatively, the relative importance of sedimentary input at each of the stations can be gauged by comparing the Mn : Al ratios observed throughout the water column with mean ratios of Mn : Al in crustal rocks (0.0034 mol mol^{-1}) (Taylor and McLennan, 1985) and Kerguelen Plateau (A3) authigenic sediments (0.011 mol mol^{-1}) (Table 2). If we divide our measured Kerguelen Plateau sediment ratio by the ratio observed at each site we obtain the fraction of authigenic sediment within each sample (Planquette et al., 2013). The sedimentary Mn : Al ratio is quite consistent between all sites (0.011–0.016) except station R-2 (0.063) (Table 2), therefore we used the sedimentary ratio at station A3 as the source signature. Chever et al. (2009) suggested that lateral transport from the northern and southern Kerguelen Plateau is a strong source to downstream stations. The mean sedimentary contribution to the Mn inventory is > 100 % at station A3 (Fig. 3), implying some degree of freshly weathered (low Mn : Al) crustal or basaltic input, in combination with sedimentary resuspension. This result supports a glacial/fluvial input or other form of bed rock weathering from Heard Island in combination with sedi-

BGD
11, 13389–13432, 2014

mentary resuspension as a source to station A3. Station R-2 had the lowest recorded mean sedimentary Mn contribution of 30 %. The recirculation-structure stations displayed mean sedimentary contributions from 40–88 %. The full water column mean sedimentary Mn contribution at station E-4E was 41 %, whereas at station E-4W (at close proximity to the Kerguelen Plateau) the observed value was 88 %.

3.8 Pseudo-Lagrangian, recirculation-structure

Station E-4W has trace metal concentrations and elemental ratios similar to A3 and will be discussed separately. However, the remaining recirculation structure stations exhibit profiles of pFe and pMn which show a minimum at approximately 150–175 m (Fig. 7). Our detailed depth profile indicates that the pFe and pMn minima coincide with the remnant winter water temperature minimum. (Fig. 8). Interestingly, Blain et al. (2014a) also estimated a winter water depth of approximately 150 m. They observed at 150 m, that nitrate and phosphate profiles within the recirculation feature, from multiple years and seasons, converged with striking consistency. Particulate Fe and pMn, concentrations increase above and below the temperature minimum, however, pAl only increases below 175 m. Particulate Al is stripped out preferentially with settling lithogenics while pFe and pMn are retained either through conversion to the biogenic particulate fraction (uptake) or adsorbed onto organic particles. It should be noted here that the work of Raiswell et al. (2011) indicates that iceberg and glacially derived Fe nanoparticulate material is typically high in Fe and low in Al. Thus, supply of glacially derived nanoparticulate Fe from Kerguelen Island, via the north east of the recirculation structure could also cause the observed high Fe, low Al surface enrichment within the recirculation structure.

Given that the pFe and pMn minima coincides with the remnant-winter-water temperature minimum, the total amount of particulate trace metals distributed throughout the winter mixed layer must be lower than during summer. This is counterintuitive if sediment resuspension is the primary source of particulate trace metals into the recirculation feature. During winter we would expect increased wind mixing, leading to more en-

BGD
11, 13389–13432, 2014

trainment of pFe over the plateau and more supply into the recirculation feature leading to a maximum at the temperature minimum. Given that we observe the inverse situation, supply into the recirculation structure must be low during winter. Thus, we suggest that the lateral supply of fluvial and glacial derived particulate trace metals must be an important source. This source would be expected to reduce in winter when precipitation as snow and glacial freezing is at a maximum and conversely, during spring, snow and ice melt and rainfall increases runoff into the coastal areas and induces a fertilisation event downstream of Heard and Kerguelen Islands. Kerguelen Island is a subantarctic island, and its climatology is cold and wet, with the Port-aux-Francais weather station recording mean daily temperatures of 2.1 °C in winter and 8.2 °C in summer and year round consistent precipitation (730 mm annually) (Meteo France). It should be noted that due to its sheltered location and sea level altitude, the Port-aux-Francais location is relatively mild compared to the west coast and interior of the island which is estimated to receive 3 times the rainfall of the east coast, or 2124 mm annually. Therefore, having a climate of high precipitation and seasonal thawing, increased seasonal runoff can be expected in spring and summer from Kerguelen Island.

The importance of fluvial sources in supplying dissolved Fe and Mn into coastal waters to the north east of Kerguelen, north of the PF, has been shown previously by Bucciarelli et al. (2001). The authors found a linear relationship between dissolved Fe and lithogenic silica and suggested that this was indicative of weathering of silicate rich minerals that characterise the Kerguelen Islands with a concomitant release of dissolved Fe and Mn. Indeed in the present study, using the lithogenic and biogenic silica data presented in Closset et al. (2014), total particulate Fe correlated significantly with total lithogenic silica ($R = 0.76$, $P < 0.01$) but not with biogenic silica. However, this significant correlation was not limited to the coastal regions in the present study and instead was observed for all stations and depths combined. Bucciarelli et al. (2001) found an exponential decrease in dissolved Fe with distance from the coast, further supporting their theory of a dominant coastal source in this region. This exponential decrease would be expected to apply to the particulate fraction also, however, it appears that

BGD
11, 13389–13432, 2014

even with an exponential decrease in pFe with distance from the coast, particulate Fe enrichment, sourced from fluvial runoff, is evident on the southern side of the PF within the recirculation feature.

The hypothesis of pFe supply from north of the PF into the eastern side of the recirculation feature via the mixing zone is supported by radium isotope data (Sanial et al., 2014) collected during the KEOPS2 mission. Apparent radium ages derived from the ratio of $^{224}Ra/^{223}Ra$ (and using the ratio observed within the Baie des Baleiniers as the starting time) suggest that the age of water since fertilisation within the recirculation feature was only 5–8 days. This indicates that there is likely rapid transfer across the PF of fertilised waters which were sourced from nearby shallow coastal areas such as the Baie des Baleiniers, Kerguelen Island. The authors go on to highlight that the heterogeneous distribution of ^{224}Ra and ^{223}Ra indicates that transfer across the polar front is sporadic in nature.

The observation of pFe enrichment in surface waters of the recirculation structure without pAl may be due to biological uptake and conversion from a bioavailable pool into the biogenic particulate pool. Alternatively or in combination, a high pFe, low pAl source such as nanoparticulate Fe characteristic of glacial/fluvial runoff (Hawkings et al., 2014; Raiswell et al., 2008a, 2006a) on Kerguelen Island could explain this observation. Indeed, temperature and salinity profiles within the recirculation structure reveal fresher and warmer water within the upper 110 m than either R-2 or A3 stations suggesting that glacial/fluvial runoff from Kerguelen Island may well be delivering this high pFe, low pAl surface enrichment.

3.9 Elemental ratios at stations E-1, E-3, E-5, E-4E and E-4W

Vertical changes in the observed elemental ratios during the pseudo-Lagrangian recirculation-structure study (Fig. 9) highlighted the influence of proximity to the fast flowing PF on E-4W, which contrasts with the other stations during the recirculation-structure study. The particles captured from the water column near station A3 have a characteristically low Mn : Fe and Ba : Al ratio in comparison to station R-2. Station

BGD
11, 13389–13432, 2014

E-4W was the closest recirculation-structure station to the Kerguelen Plateau and appeared to be influenced by sedimentary sources having Mn : Fe and Ba : Al ratios much closer to A3 than any other recirculation-structure station. The profiles of trace metals within the recirculation structure (Fig. 7) also highlighted unusually high pFe and pAl at station E4-W, which further supports the hypothesis that E-4W was very similar to A3 in its trace metal inventory and most likely had a similar source. Trull et al. (2014) analysed surface water community size structure based on chemical and isotopic measurements and also revealed many similarities between stations A3 and E-4W and resulted in the authors grouping these stations together and separate from the remaining recirculation structure stations.

Conversely, E-4E, which is the recirculation-structure station at the greatest distance from the Kerguelen Plateau, had elemental ratios below the mixed layer similar to station R-2 (Table 4). The particulate trace metal inventory observed at station E-4E we believe has originated from modified HNLC-type water in the vicinity of the Leclaire Rise. The remaining recirculation-structure stations (E-1, E-3, E-5) appear to have source signatures reflecting intermediate elemental ratios between the two unique end-member stations, E-4W and E-4E, and indicates a degree of mixing between these two unique sources. Interestingly, below the depth of the winter water temperature minimum of 150–175 m, we observe striking consistency in the elemental ratios of pFe : pAl and pMn : pAl. This suggests that the particles distributed throughout the water column below approximately 175 m have a similar composition and therefore source.

4 Conclusions

This study has identified two distinct areas of Fe fertilisation in the vicinity of Kerguelen Island. Firstly, the plateau itself is a major source of resuspended shelf sediments to station A3 especially below the mixed layer. Secondly, fluvial and glacial runoff into coastal waters in combination with resuspension of shallow coastal sediments fertilises areas to the north of the PF, east of Kerguelen Island, but also across the PF and into

BGD
11, 13389–13432, 2014

the recirculation feature from the north-east. Indications of particle transport across the PF were observed at station R-2 sourced from the Leclaire Rise to the north of the PF. Satellite imagery also revealed filaments clearly diverging from the main jet of the PF and into the north east of the recirculation structure. Within the recirculation structure, the correspondence of the winter water temperature minimum with the particulate trace metal minimum implies that a seasonal cycle is involved in the supply of trace elements. This is most likely driven by increased fluvial and glacial runoff in summer, associated with rainfall and basal melt and reduced supply in winter when snowfall and freezing conditions predominate. In this complex region, it appears that weathering of the islands themselves are direct sources of new Fe and help stimulate the seasonal bloom that is significant in terms of the regional carbon cycle.

Over the mesoscale, it appears that physical processes associated with settling of refractory lithogenic particles was an important process in modifying the particulate elemental ratios. However, on the individual profile scale, biological processes seem important in modifying the elemental ratios in surface waters through preferential uptake of bio-essential elements, even from the particulate fraction.

Repeat sampling over the plateau provided a perspective on the persistence of the particulate Fe availability. Small particles containing pFe were efficiently transported out of the mixed layer during a bloom event over stations A3. This resulted in a 70 % reduction in the integrated pFe stock within the mixed layer as a result of physical aggregation of small particles onto phyto-aggregates, presumably decreasing particle buoyancy and increasing export out of the mixed layer. This is likely to be an important aspect of the complex interaction between iron supply and biological availability, capable of mediating bloom duration and thus the efficiency of carbon sequestration.

Acknowledgements. This work was supported by the Antarctic Climate and Ecosystems Cooperative Research Centre, University of Tasmania, Australia. This work was also supported by the French Research program of INSU-CNRS LEFE-CYBER (Les enveloppes fluides et l'environnement –Cycles biogéochimiques, environnement et ressources), the French ANR (Agence Nationale de la Recherche, SIMI-6 program, ANR-10-BLAN-0614), the French CNES (Centre National d'Etudes Spatiales) and the French Polar Institute IPEV (Institut Polaire Paul-

BGD
11, 13389–13432, 2014

Emile Victor). We would like to thank the captain and the crew of the R.V. *Marion Dufresne*, Stephane Blain and Bernard Quéguiner as chief scientist and project coordinator of the KEOPS2 cruises, respectively. Leanne Armand was supported by grant Australian Antarctic Division, AAS grant #3214. Access to Sector Field ICP-MS instrumentation was supported through ARC LIEF funding (LE0989539).

References

Angino, E.: Geochemistry of Antarctic pelagic sediments, Geochim. Cosmochim. Acta, 30, 939–961, 1966.

Angino, E. and Andrews, R.: Trace element chemistry, heavy minerals, and sediment statistics of Weddell Sea sediments, J. Sediment. Res., 38, 634–642, 1968.

Armand, L. K., Crosta, X., Quéguiner, B., Mosseri, J., and Garcia, N.: Diatoms preserved in surface sediments of the northeastern Kerguelen Plateau, Deep-Sea Res. Pt. II, 55, 677–692, 2008.

Blain, S., Queguiner, B., Armand, L., Belviso, S., Bombled, B., Bopp, L., Bowie, A. R., Brunet, C., Brussaard, C., Carlotti, F., Christaki, U., Corbiere, A., Durand, I., Ebersbach, F., Fuda, J. L., Garcia, N., Gerringa, L., Griffiths, B., Guigue, C., Guillerm, C., Jacquet, S. H. M., Jeandel, C., Laan, P., Lefevre, D., Lo Monaco, C., Malits, A., Mosseri, J., Obernosterer, I., Park, Y. H., Picheral, M., Pondaven, P., Remenyi, T., Sandroni, V., Sarthou, G., Savoye, N., Scouarnec, L., Souhaut, M., Thuiller, D., Timmermans, K., Trull, T., Uitz, J., Van Beek, P., Veldhuis, M., Vincent, D., Viollier, E., Vong, L., and Wagener, T.: Effect of natural iron fertilization on carbon sequestration in the Southern Ocean, Nature, 446, 1070–1074, 2007.

Blain, S., Capparos, J., Guéneuguès, A., Obernosterer, I., and Oriol, L.: Distributions and stoichiometry of dissolved nitrogen and phosphorus in the iron fertilized region near Kerguelen (Southern Ocean), Biogeosciences Discuss., 11, 9949–9977, doi:10.5194/bgd-11-9949-2014, 2014a.

Blain, S., Quéguiner, B., Trull, T., Boutin, J., Bowie, A. R., Cavagna, A. J., Carlotti, F., Christaki, U., Chever, F., Closset, I., Dehairs, F., d'Ovidio, F., Fernandez, C., Fourquez, M., Jouandet, M., Lasbleiz, M., Leblanc, K., Monaco, C., Laurenceau, E., Metzl, N., Lefèvre, D., Obernosterer, I., Park, Y., Planchon, F., Quéroué, F., Sallée, J-B., Sarthou, G., van der Merwe, P.,

BGD
11, 13389–13432, 2014

Van-Beek, P., and Zhou, M.: Large scale assessment of natural iron fertilization in the Southern Ocean, Nature, submitted, 2014b.
Bopp, L., Kohfeld, K. E., Le Quéré, C., and Aumont, O.: Dust impact on marine biota and atmospheric CO_2 during glacial periods, Paleoceanography, 18, 1–24, 2003.
Bowie, A. R., Townsend, A. T., Lannuzel, D., Remenyi, T. A., and van der Merwe, P.: Modern sampling and analytical methods for the determination of trace elements in marine particulate material using magnetic sector inductively coupled plasma-mass spectrometry. Anal. Chim. Acta, 676, 15–27, 2010.
Bowie, A. R., van der Merwe, P., Trull, T., Quéroué, F., Fourquez, M., Planchon, F., Sarthou, G., and Blain, S.: Iron budgets for three distinct biogeochemical sites around the Kerguelen plateau (Southern Ocean) during the natural fertilization experiment KEOPS-2, Biogeosciences Discuss., 2014.
Boyd, P. W., Jickells, T., Law, C. S., Bowie, A. R., Boyle, E. A., Buesseler, K. O., Coale, K. H., Cullen, J. J., de Baar, H. J. W., Follows, M., Harvey, M., Lancelot, C., Levasseur, M., Owens, N. P. J., Pollard, R., Rivkin, R. B., Sarmiento, J., Schoemann, V., Smetacek, V., Takeda, S., Tsuda, A., Turner, S., and Watson, A. J.: Mesoscale iron enrichment experiments 1993–2005: synthesis and future directions, Science, 315, 612–617, 2007.
Bucciarelli, E., Bowie, A. R., and Tréguer, P.: Iron and manganese in the wake of the Kerguelen Islands (Southern Ocean), Mar. Chem., 73, 21–36, 2001.
Chever, F., Sarthou, G., Bucciarelli, E., and Bowie, A. R.: An iron budget during the natural iron fertilisation experiment KEOPS (Kerguelen Islands, Southern Ocean), Biogeosciences, 7, 455–468, 2009, http://www.biogeosciences.net/7/455/2009/.
Closset, I., Lasbleiz, M., Leblanc, K., Quéguiner, B., Cavagna, A.-J., Elskens, M., Navez, J., and Cardinal, D.: Seasonal evolution of net and regenerated silica production around a natural Fe-fertilized area in the Southern Ocean estimated from Si isotopic approaches, Biogeosciences Discuss., 11, 6329–6381, doi:10.5194/bgd-11-6329-2014, 2014.
Cullen, J. T. and Sherrell, R. M.: Techniques for determination of trace metals in small samples of size-fractionated particulate matter: phytoplankton metals off central California, Mar. Chem., 67, 233–247, 1999.
De Baar, H. J. W.: Synthesis of iron fertilization experiments: from the Iron Age in the Age of Enlightenment, J. Geophys. Res., 110, C09S16, doi:10.1029/2004JC002601, 2005.

BGD
11, 13389–13432, 2014

De Baar, H. J. W. and de Jong, J. T.: Distribution, sources and sinks of iron in seawater, in: The Biogeochemistry of Iron in Seawater, edited by: Turner, D. R. and Hunter, K. A., IUPAC Series on Analytical and Physical Chemistry of Environmental Systems, 123–253, 2001.

Doucet, S., Scoates, J. S., Weis, D., and Giret, A.: Constraining the components of the Kerguelen mantle plume: a Hf-Pb-Sr-Nd isotopic study of picrites and high-MgO basalts from the Kerguelen Archipelago, Geochem. Geophy. Geosy., 6, Q04007, doi:10.1029/2004GC000806, 2005.

Frew, R. D., Hutchins, D. A., Nodder, S., Sanudo-Wilhelmy, S., Tovar-Sanchez, A., Leblanc, K., Hare, C. E., and Boyd, P. W.: Particulate iron dynamics during Fe cycle in sub-antarctic waters southeast of New Zealand, Global Biogeochem. Cy., 20, GB1S93, doi:10.1029/2005GB002558, 2006.

German, C., Campbell, A., and Edmond, J.: Hydrothermal scavenging at the Mid-Atlantic Ridge: modification of trace element dissolved fluxes, Earth Planet. Sci. Lett., 107, 101–114, 1991.

Hawkings, J. R., Wadham, J. L., Tranter, M., Raiswell, R., Benning, L. G., Statham, P. J., Tedstone, A., Nienow, P., Lee, K., and Telling, J.: Ice sheets as a significant source of highly reactive nanoparticulate iron to the oceans, Nat. Commun., 5, 3929, doi:10.1038/ncomms4929, 2014.

Johnson, K. S., Gordon, R. M., and Coale, K. H.: What controls dissolved iron concentrations in the world ocean?, Mar. Chem., 57, 137–161, 1997.

Jouandet, M.-P., Jackson, G. A., Carlotti, F., Picheral, M., Stemmann, L., and Blain, S.: Rapid formation of large aggregates during the spring bloom of Kerguelen Island: observations and model comparisons, Biogeosciences, 11, 4393–4406, doi:10.5194/bg-11-4393-2014, 2014.

Lasbleiz, M., Leblanc, K., Blain, S., Ras, J., Cornet-Barthaux, V., Hélias Nunige, S., and Quéguiner, B.: Pigments, elemental composition (C, N, P, Si) and stoichiometry of particulate matter, in the naturally iron fertilized region of Kerguelen in the Southern Ocean, Biogeosciences Discuss., 11, 8259–8324, doi:10.5194/bgd-11-8259-2014, 2014.

Laurenceau, E. C., Trull, T., Davies, D. M., Bray, S. G., Doran, J., Planchon, F., Cavagna, A.-J., and Waite, A.: The relative importance of phytodetrital aggregates and fecal matter in the control of export fluxes from naturally iron-fertilised waters near the Kerguelen plateau, Biogeosciences Discuss., 2014.

Martin, J. H.: Glacial–interglacial CO_2 change: the iron hypothesis, Paleoceanography, 5, 1–13, 1990.

BGD
11, 13389–13432, 2014

McCave, I. N.: Local and global aspects of the bottom nepheloid layers in the world ocean, Netherlands J. Sea Res., 20, 167–181, 1986.
Moffett, J. W.: Transformations among different forms of iron in the ocean, in: The Biogeochemistry of Iron in Seawater, edited by: Turner, D. R. and Hunter, K. A., John Wiley & Sons, New York, 343–372, 2001.
Park, Y.-H., Roquet, F., Durand, I., and Fuda, J.-L.: Large-scale circulation over and around the Northern Kerguelen Plateau, Deep-Sea Res. Pt. II, 55, 566–581, 2008.
Planchon, F., Ballas, D., Cavagna, A.-J., Bowie, A. R., Davies, D. M., Trull, T., Laurenceau, E. C., van der Merwe, P., and Dehairs, F.: Carbon export in the naturally iron-fertilized Kerguelen area of the Southern Ocean based on the ^{234}Th approach, Biogeosciences Discuss., 2014.
Planquette, H., Sherrell, R. M., Stammerjohn, S., and Field, M. P.: Particulate iron delivery to the water column of the Amundsen Sea, Antarctica, Mar. Chem., 153, 15–30, 2013.
Pollard, R., Salter, I., Sanders, R., and Lucas, M.: Southern Ocean deep-water carbon export enhanced by natural iron fertilization, Nature, 457, 577–581, 2009.
Poulton, S. W. and Raiswell, R.: Chemical and physical characteristics of iron oxides in riverine and glacial meltwater sediments, Chem. Geol., 218, 203–221, 2005.
Quéguiner, B.: Iron fertilization and the structure of planktonic communities in high nutrient regions of the Southern Ocean, Deep-Sea Res. Pt. II, 90, 43–54, 2013.
Quéroué, F., Sarthou, G., Chever, F., van der Merwe, P., Lannuzel, D., Townsend, A. T., Bucciarelli, E., Planquette, H., Cheize, M., Blain, S., d'Ovidio, F., Bowie, A. R.: A new study of natural Fe fertilization processes in the vicinity of the Kerguelen Islands (KEOPS2 experiment), Biogeosciences Discuss., 2014.
Raiswell, R.: Iceberg-hosted nanoparticulate Fe in the Southern Ocean: mineralogy, origin, dissolution kinetics and source of bioavailable Fe, Deep-Sea Res. Pt. II, 58, 1364–1375, 2011.
Raiswell, R., Tranter, M., Benning, L. G., Siegert, M., De'ath, R., Huybrechts, P., and Payne, T.: Contributions from glacially derived sediment to the global iron (oxyhydr)oxide cycle: implications for iron delivery to the oceans, Geochim. Cosmochim. Acta, 70, 2765–2780, 2006.
Raiswell, R., Benning, L. G., Davidson, L., and Tranter, M.: Nanoparticulate bioavailable iron minerals in icebergs and glaciers, Mineral. Mag., 72, 345–348, 2008a.
Raiswell, R., Benning, L. G., Tranter, M., Tulaczyk, S.: Bioavailable iron in the Southern Ocean: the significance of the iceberg conveyor belt, Geochem. Trans., 9, doi:10.1186/1467-4866-9-, 2008b.

BGD
11, 13389–13432, 2014

Raiswell, R., Vu, H. P., Brinza, L., Benning, L. G.: The determination of labile Fe in ferrihydrite by ascorbic acid extraction: methodology, dissolution kinetics and loss of solubility with age and de-watering, Chem. Geol., 278, 70–79, 2010.

Sanial, V., van Beek, P., Lansard, B., Souhaut, M., Kestenare, E., d'Ovidio, F., and Blain, S.: Use of Ra isotopes to deduce rapid transfer of sediment-derived inputs off Kerguelen, Biogeosciences Discuss., 2014.

Savoye, N., Trull, T., Jacquet, S. H. M., Navez, J., and Dehairs, F.: ^{234}Th-based export fluxes during a natural iron fertilization experiment in the Southern Ocean (KEOPS), Deep-Sea Res. Pt. II, 55, 841–855, 2008.

Schroth, A. W., Crusius, J., Sholkovitz, E. R., and Bostick, B. C.: Iron solubility driven by speciation in dust sources to the ocean, Nat. Geosci., 2, 337–340, 2009.

Shaw, T. J., Raiswell, R., Hexel, C. R., Vu, H. P., Moore, W. S., Dudgeon, R., and Smith, K. L.: Input, composition, and potential impact of terrigenous material from free-drifting icebergs in the Weddell Sea, Deep-Sea Res. Pt II, 58, 1376–1383, 2011.

Shigemitsu, M., Nishioka, J., Watanabe, Y. W., Yamanaka, Y., Nakatsuka, T., and Volkov, Y. N.: Fe/Al ratios of suspended particulate matter from intermediate water in the Okhotsk Sea: implications for long-distance lateral transport of particulate Fe, Mar. Chem., 157, 41–48, 2013.

Sunda, W. G.: Bioavailability and bioaccumulation of iron in the sea, in: The Biogeochemistry of Iron in Seawater, edited by: Turner, D. R. and Hunter, K. H., IUPAC Series on Analytical and Physical Chemistry of Environmental Systems, 41–84, 2001.

Taylor, S. R., McLennan, S. M., and Scott, M.: The Continental Crust, its Composition and Evolution?: an Examination of the Geochemical Record Preserved in Sedimentary Rocks, Blackwell Scientific Publications, Oxford, Melbourne, 1985.

Townsend, A. T.: The accurate determination of the first row transition metals in water, urine, plant, tissue and rock samples by sector field ICP-MS, J. Anal. At. Spectrom., 15, 307–314, 2000.

Trull, T., Davies, D. M., Dehairs, F., Cavagna, A.-J., Lasbleiz, M., Laurenceau, E. C., D'Ovidio, F., Planchon, F., Queguiner, B., and Blain, S.: Chemometric perspectives on plankton community responses to natural iron fertilization over and downstream of the Kerguelen plateau in the Southern Ocean, Biogeosciences Discuss., 2014.

BGD
11, 13389–13432, 2014

Twining, B. S., Baines, S. B., and Fisher, N. S.: Element stoichiometries of individual plankton cells collected during the Southern Ocean Iron Experiment (SOFeX), Limnol. Oceanogr., 49, 2115–2128, 2004.

Van Beek, P., Bourquin, M., Reyss, J. L., Souhaut, M., Charette, M. A., and Jeandel, C.: Radium isotopes to investigate the water mass pathways on the Kerguelen Plateau (Southern Ocean), Deep-Sea Res. Pt. II, 55, 622–637, 2008.

Watson, A. J., Bakker, D. C. E., Ridgwell, A. J., Boyd, P. W., and Law, C. S.: Effect of iron supply on Southern Ocean CO_2 uptake and implications for glacial atmospheric CO_2, Nature, 407, 730–733, doi:10.1038/35037561, 2000.

Zhang, Y., Lacan, F., and Jeandel, C.: Dissolved rare earth elements tracing lithogenic inputs over the Kerguelen Plateau (Southern Ocean), Deep-Sea Res. Pt. II, 55, 638–652, 2008.

Zhou, M., Zhu, Y., d'Ovidio, F., Park, Y.-H., Durand, I., Kestenare, E., Sanial, V., Van-Beek, P., Queguiner, B., Carlotti, F., and Blain, S.: Surface currents and upwelling in Kerguelen Plateau regions, Biogeosciences Discuss., 11, 6845–6876, doi:10.5194/bgd-11-6845-2014, 2014.

BGD
11, 13389–13432, 2014

Table 1. KEOPS2 sampling locations and station types.

	A3–1	A3–2	R-2	F-L	E-1	E-3	E-5	E-4E	E-4W
Station type	Kerguelen Plateau 1st visit	Kerguelen Plateau 2nd visit	HNLC reference station	Northern Polar Front	Recirculation structure	Recirculation structure	Recirculation structure	Eastern recirculation structure	Western recirculation structure
Sampling date	20 Oct 2011	16 Nov 2011	25 Oct 2011	6 Nov 2011	29 Oct 2011	3 Nov 2011	18 Nov 2011	13 Nov 2011	11 Nov 2011
Latitude (S)	50°37.7574′	50°37.4306′	50°21.52′	48°31.394′	48°29.5728′	48°42.1334′	48°24.698′	48°42.9218′	48°45.927′
Longitude (E)	72°4.8193′	72°3.3366′	66°43.00′	74°40.036′	72°14.1467′	71°58.0027′	71°53.7894′	72°33.7792′	71°25.51′
Bottom depth (m)	505	505	2528	2690	2050	1910	1920	2200	1400
Time series	Yes	Yes	No	No	Yes	Yes	Yes	No	No
Particulate Trace Metals	Yes	Yes	Yes	Yes	Yes	Yes	Yes	Yes	Yes
POC PON	Yes	Yes	Yes	Yes	Yes	Yes	Yes	Yes	Yes
Sediment samples	Yes	Yes	Yes	Yes	No	Yes	No	Yes	Yes
Sediment trap samples	No	Yes	No	No	Yes	Yes	Yes	No	No

BGD
11, 13389–13432, 2014

Table 2. Mean elemental ratios of authigenic sediments at each station.

Station	pFe : pAl	pMn : pAl	pMn : pFe	pBa : pAl
TEW1	1.10	0.013	0.012	0.003
E3	0.93	0.015	0.016	0.125
E4W	0.81	0.013	0.016	0.013
R2	0.73	0.063	0.086	0.892
A3	0.87	0.011	0.013	0.026
FL	0.82	0.016	0.019	0.040
Kerguelen Archipelago Basalts (Doucet et al., 2005)	0.77–1.4	0.011–0.045	0.013–0.014	0.0014–0.0024

BGD
11, 13389–13432, 2014

Table 3. Mean elemental ratios of marine snow particles captured in free-floating sediment traps.

Station	pFe : pAl	pMn : pAl	pFe : pMn	pBa : pAl
E-1	1.02	0.009	113	0.16
E-3	1.05	0.010	105	0.28
E-5	0.91	0.008	112	0.32
A3-2	0.70	0.008	88	0.03

BGD
11, 13389–13432, 2014

Table 4. Mean elemental ratios of particulate matter (1–53 µm) below the mixed layer at each station.

Station	pBa : pAl	pMn : pAl	pFe : pAl	pMn : pFe
A3-1	0.027	0.007	0.53	0.013
A3-2	0.034	0.009	0.63	0.014
R-2	0.322	0.036	0.65	0.059
F-L	0.190	0.020	0.77	0.027
E-4E	0.383	0.037	0.86	0.045
E-4W	0.078	0.014	0.63	0.021
E-1	0.185	0.023	0.68	0.034
E-3	0.258	0.024	0.71	0.033
E-5	0.260	0.020	0.68	0.030

BGD
11, 13389–13432, 2014

Table A1. Percentage recoveries of BCR-414 certified reference material. Certified and single lab values taken from the final report of the Commission of the European Communities, Community Bureau of Reference for BCR-414, EUR14558.

mg kg^{-1}	Rep 1	Rep 2	Rep 3	Mean	SD	RSD (%)	Certified	% Recovery	Single lab analysis	% Recovery
Ba	34	26	32	31	4.0	13.1			31	99
Al	2243	1349	1943	1845	454.6	24.6			1800	102
Mn	278	284	283	282	3.4	1.2	299	94		
Fe	1874	1850	1878	1867	15.0	0.8	1850	101		

BGD
11, 13389–13432, 2014

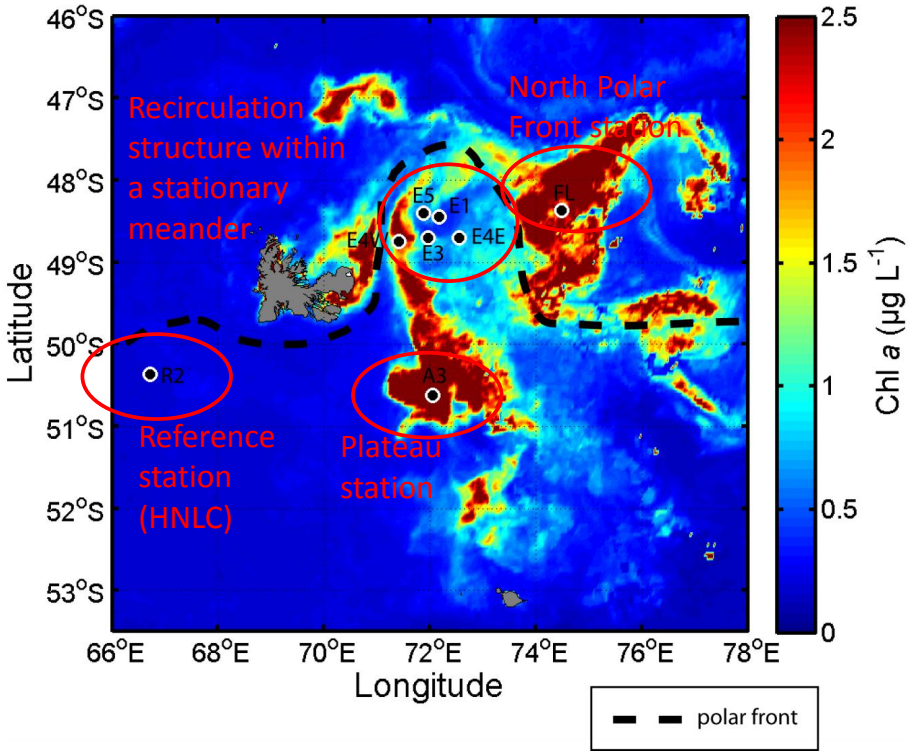

SeaWiFS files courtesy of CLS (with support from CNES)

Figure 1. SeaWiFS surface chlorophyll on the 11 November 2011, approximately half way through the KEOPS2 sampling program. Kerguelen and Heard Island are visible in grey. Stations that were sampled for suspended particles are indicated with black circles. Distinct regimes of interest for the KEOPS2 program are indicated in red.

BGD
11, 13389–13432, 2014

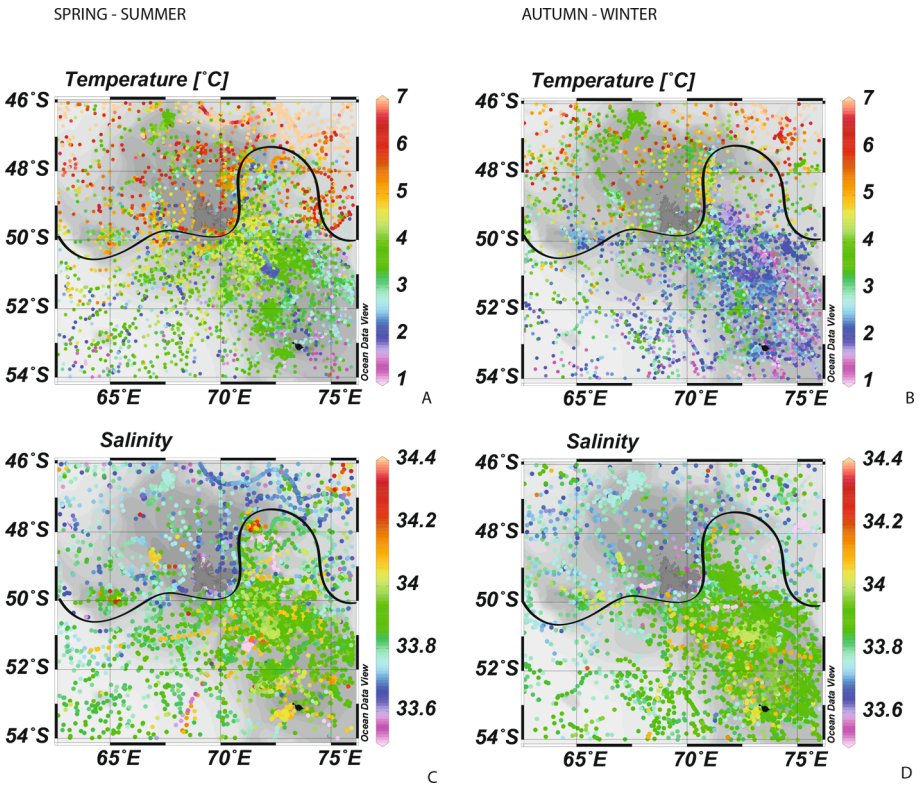

Figure 2. Surface (10 m) temperature in Spring–Summer **(A)** and Winter–Autumn **(B)** as well as surface salinity in Spring–Summer **(C)** and Winter–Autumn **(D)** within the study area from 1970 until 2013. The PF is identified as a solid black line. Kerguelen and Heard Island are visible in dark grey and black respectively and the Leclaire Rise can be identified as the shallow bathymetry, north of the PF, near the western boundary of the map. Data obtained from the World Ocean Database (http://www.nodc.noaa.gov).

BGD
11, 13389–13432, 2014

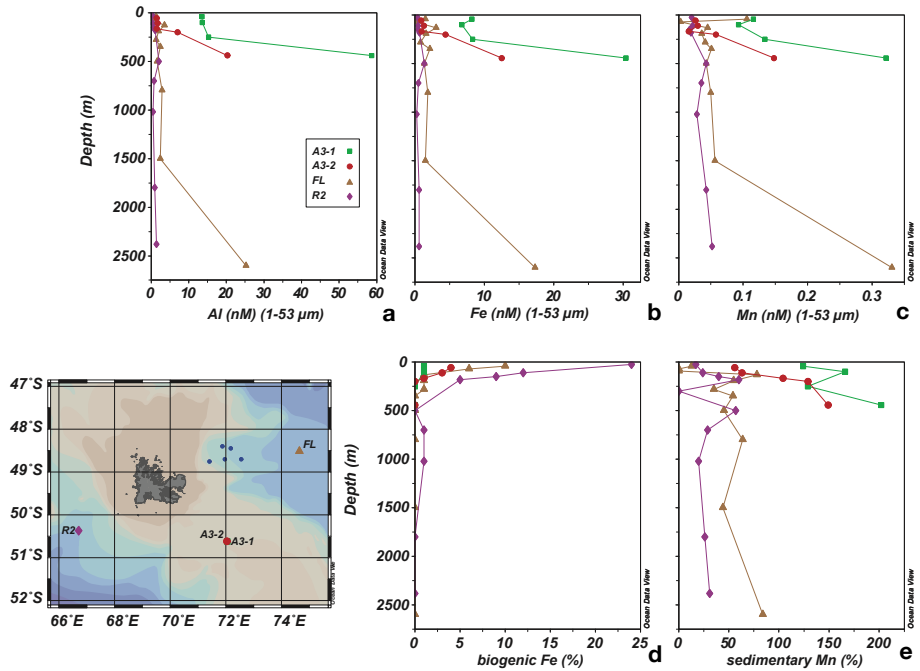

Figure 3. Profiles of particulate Al**(a)**, Fe**(b)** and Mn **(c)** (1–53 µm) at the reference HNLC station (R-2), the northern PF station (F-L) and pre and post-bloom over the plateau station, highlighting the contrasting particulate trace metal supply to these locations. Profiles of biogenic Fe **(d)** and sedimentary Mn **(e)** are given to highlight the source to each station (see text for details). Biogenic Fe (as a percentage of the total Fe) in surface waters shows a clear progression that can be explained by the location of each station within the study area whereby, biogenic Fe at R-2 ≫ F-L > A3–2 > A3–1. Sedimentary Mn values greater than 100 % indicate a source signature with low Mn : Al such as bedrock (0.0034).

BGD
11, 13389–13432, 2014

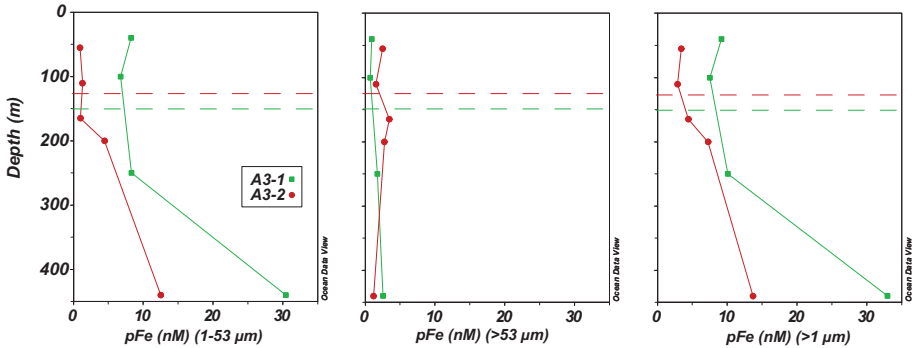

Figure 4. Particulate Fe at the plateau station (A3) by size class. The integrated full water column pFe (> 1 µm) reduced by 51 % between A3–1 and A3–2 (9.1–4.5 mMol m^{-2} at A3–1 and A3–2 respectively). The integrated mixed layer pFe reduced by 70 % between A3–1 and A3–2 (1.4–0.56 mMol m^{-2} at A3–1 and A3–2, respectively). The mixed layer shoaled between A3–1 and A3–2 as illustrated by the dashed horizontal line. The calculation of integrated mixed layer pFe used a constant mixed layer depth of 165 m for both A3–1 and A3–2 to allow comparison between these stations.

BGD
11, 13389–13432, 2014

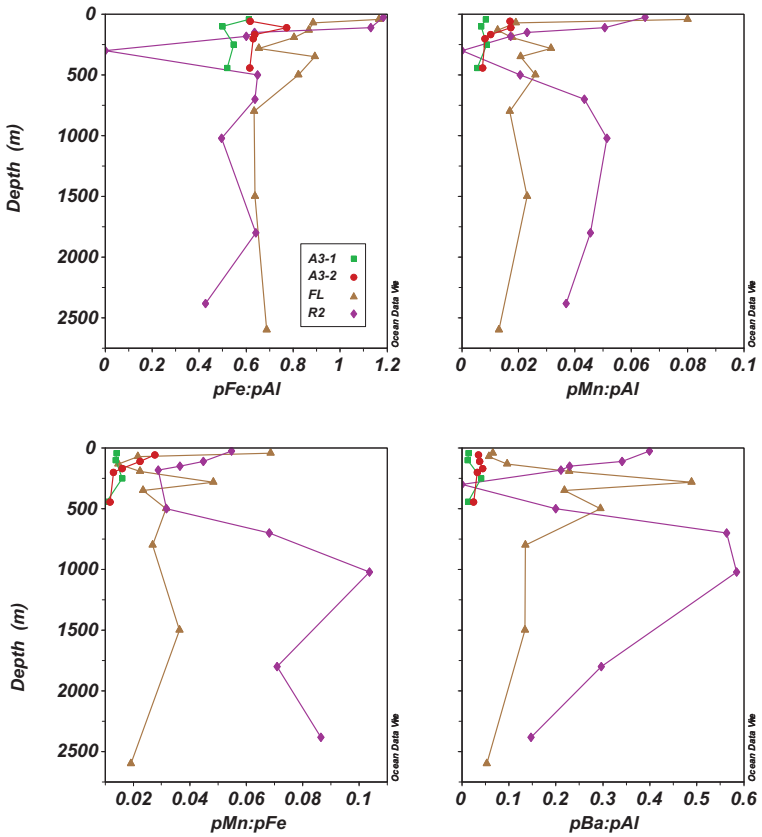

Figure 5. Profiles of elemental ratios at the reference station (R-2), northern PF (F-L) and pre and post-bloom over the plateau station. Note the increase in pMn and pBa relative to pAl at station R-2 below 500 m.

BGD
11, 13389–13432, 2014

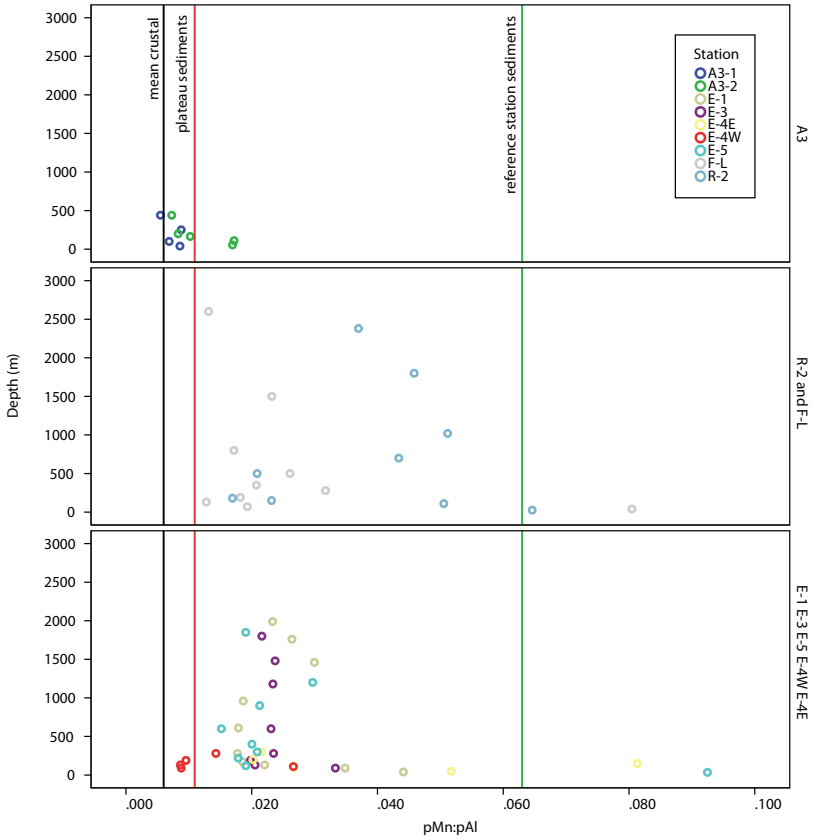

Figure 6. Ratio of pMn : pAl vs. depth, separated by station type. Vertical lines represent the mean crustal ratio (black), authigenic Kerguelen Plateau sediments (red) and station R-2 authigenic sediments (green).

BGD
11, 13389–13432, 2014

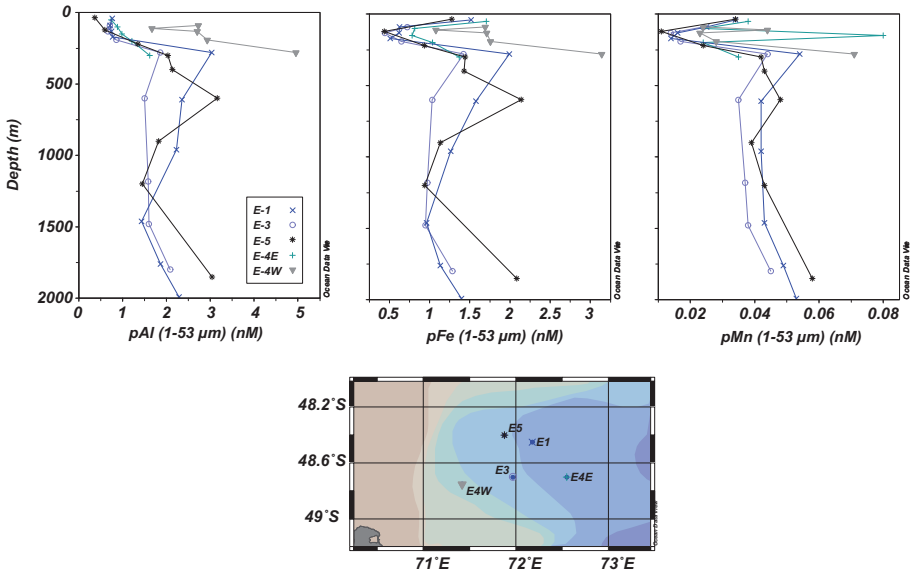

Figure 7. Profiles of particulate trace metals during the pseudo-lagrangian recirculation-structure study. Station E-4W exhibits unique trace metal profiles in comparison to the remaining stations (see text for details). Note the distinct pFe and pMn minima at 150–175 m. Particulate Al exhibits a similar profile albeit without surface enrichment.

BGD
11, 13389–13432, 2014

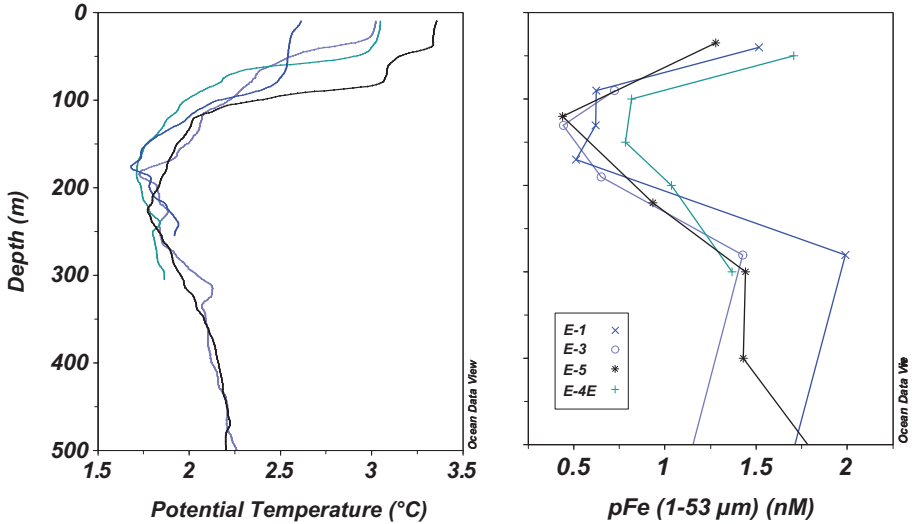

Figure 8. Temperature profiles within the upper 500 m within the recirculation structure are shown alongside corresponding profiles of particulate Fe (1–53 µm) within the upper 500 m within the recirculation structure.

BGD
11, 13389–13432, 2014

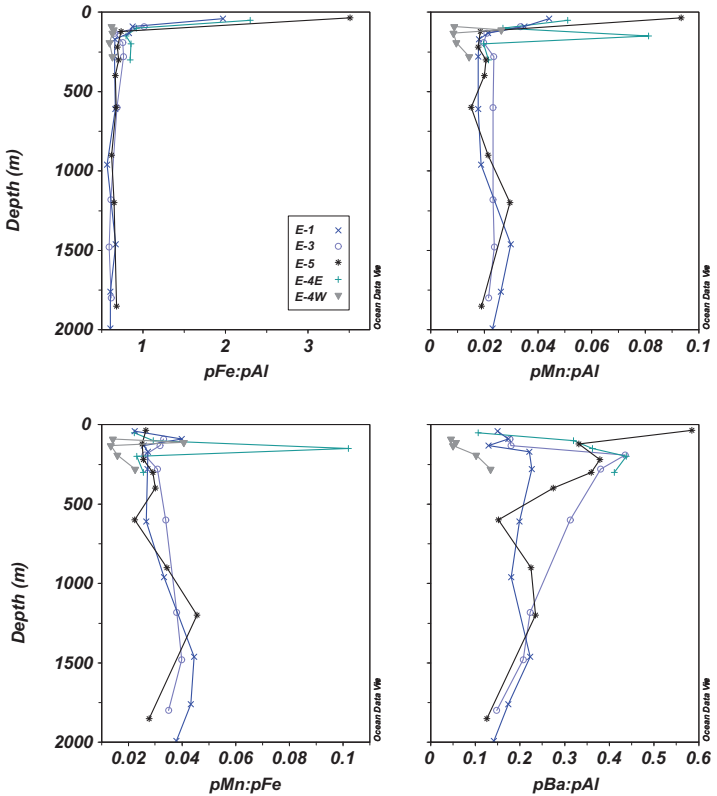

Figure 9. Profiles of elemental ratios during the pseudo-lagrangian recirculation-structure study. Stations E-1, E-3 and E-5 can be considered a pseudo-lagrangian time series, while stations E-4W and E-4E are situated at the western and eastern extremes of the recirculation structure. Note the relative consistency in various elemental ratios below the winter water temperature minimum depth of 150–175 m.

BGD
11, 13389–13432, 2014